Intracellular Expression of a Fluorogenic DNA Aptamer Using Retron Eco2

Mahesh A. Vibhute, Corbin Machatzke, Katrin Bigler, Saskia Krümpel, Daniel Summerer and Hannes Mutschler*

Department of Chemistry and Chemical Biology, TU Dortmund University, Otto-Hahn-Str. 4a, 44227 Dortmund

Correspondence to: hannes.mutschler@tu-dortmund.de

DNA aptamers are short, single-stranded DNA molecules that bind specifically to a range of targets such as proteins, cells, and small molecules. Typically, they are utilized in the development of therapeutic agents, diagnostics, drug delivery systems, and biosensors. Although aptamers perform well in controlled extracellular environments, their intracellular use has been less explored due to challenges of expressing them in vivo. In this study, we employed the bacterial retron system Eco2, to express a DNA light-up aptamer in *Escherichia coli*. Both in vitro and in vivo assays confirm that structure-guided insertion of the aptamer domain into the non-coding region of the retron enables reverse transcription and folding of functional aptamer constructs in vivo. Notably, we find only a limited correlation between in vitro and in vivo aptamer performance, suggesting marked folding differences between the two environments. Our findings demonstrate that retrons can be used to effectively express short DNA aptamers within living cells, potentially broadening and optimizing their application in intracellular settings.

Introduction

Aptamers are single stranded nucleic acids that fold into distinct structures, allowing them to bind specifically to target ligands.[1] The ligand-binding sites of aptamers are tailored to the shape and charge of the ligand, enabling precise interactions. In particular, aptamers isolated through in vitro selection protocols serve as affinity reagents, positioning them as nucleic acid analogues of antibodies.[2,3] As such, they offer distinct advantages over their protein-based counterparts such as small size, as

well as rapid and cost-effective manufacturing.[3] An area of particular interest is the development of fluorescent light-up aptamers (FLAPs),[4–6] which specifically bind conditionally fluorescent dyes and activate their fluorescence.[7] The advent of FLAPs has also significantly advanced the study of folding of aptamers, as efficient folding can be determined as a function of fluorescence output. Pioneering work by Jaffery and coworkers has led to proliferation of numerous FLAPS. Notable examples include the RNA-FLAPs Spinach[8], Broccoli[9], Corn[10], Mango[11], Squash[12] and Pepper[7]. These FLAPs serve as RNA mimics of fluorescent proteins and have transformed cellular imaging techniques to locate and understand RNA dynamics in vivo.

In contrast to RNA aptamers, DNA aptamers offer enhanced stability, greater ease of synthesis and chemical modification, as well as reduced cost, thereby facilitating more straightforward production and broader applicability in diverse fields, including therapeutics and diagnostics.[3,13] For example Lettuce, a DNA FLAP that mimics the fluorescent properties of GFP holds great promise for in pathogen detection or as intracellular sensors for tumor cell recognition.[14–16] However, since most DNA aptamer studies focus on their development and characterization in vitro, their potential for applications inside living cells remains largely unexplored. A particular challenge in this context is the difficulty of biosynthesising DNA aptamers in cells. Indeed, the ability to transcribe single-stranded RNA from DNA-based vectors has decisively contributed to the development of diverse RNA FLAPs for in-cell applications, such as the Broccoli aptamer[9]. Therefore, methods for the intracellular synthesis and functional studies of single-stranded DNA (ssDNA) aptamers, is highly desirable. Only a few approaches for intracellular ssDNA synthesis have been reported, in all cases using exogeneous systems such as phagemid vectors[17], phages[18] and retroviral reverse transcriptases[19–23].

A more integrated, efficient, and potentially safer alternative to exogenous ssDNA expression systems could be the use of endogenous bacterial platforms such as retrons. Retrons are prokaryotic elements that are thought to contribute to defense against phage infection.[24–27] Each retron typically consists of three components, namely a ncRNA transcript, an RT, and an effector protein. The ncRNA transcript adopts a specific secondary structure, nested between two repeat regions at its 5’ and 3’ end that are complementary and hybridize (Figure 1). The RT recognizes the

folded ncRNA and initiates reverse transcription from the 2'OH of a conserved guanosine, using the base-paired region as primer.[28] The reverse transcription proceeds until about halfway along the ncRNA. Simultaneously, the RNA template is degraded by RNase H1, except for a stretch of approximately 5-10 RNA bases, which remain hybridized to the cDNA.[24] This results in a hybrid RNA-DNA structure (RT-DNA), with the non-coding RNA and DNA elements *msr* and *msd*, respectively. *msr* and *msd* are covalently attached by a 2'-5' linkage at the conserved guanosine and the base paired region close to the 5' end of *msd* (3' end of *msr*). This ability of retrons to synthesize abundant ssDNA in vivo has generated considerable interest in using them as an alternative to exogenously delivered DNA oligonucleotides in genome engineering and genome editing.[28–35]

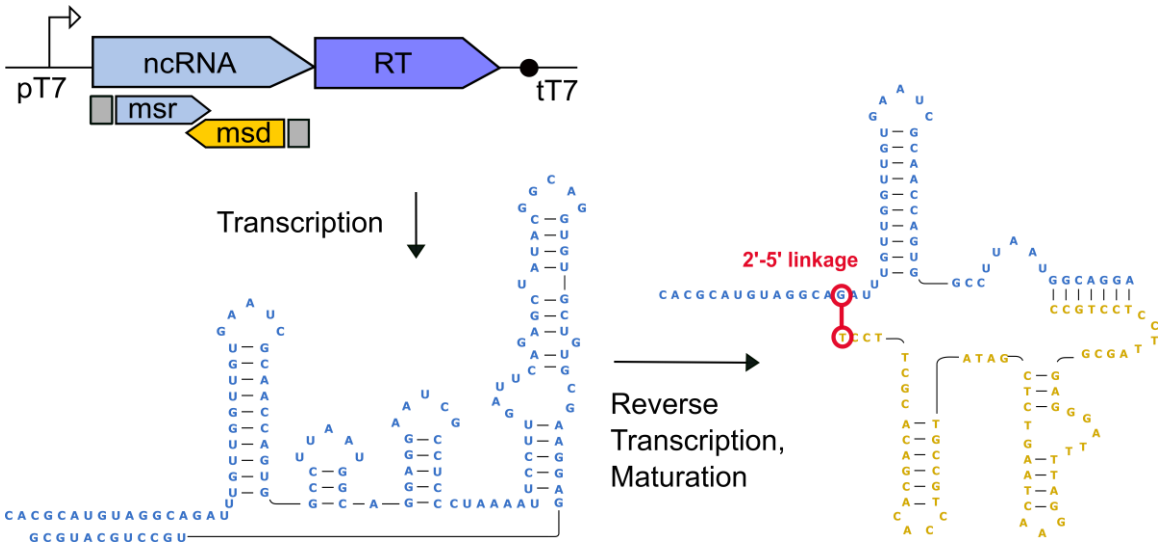

Figure 1. Schematic of DNA template, ncRNA and the RT-DNA. The ncRNA is indicated in blue, the terminal 5' and 3' repeats are shown in grey. The *msd* region which is reverse transcribed is indicated in yellow. The conserved guanosine and 2'-5' linkage are highlighted in red.

While retrons have also been proposed as a potential method for expressing DNA aptamers,[20,22] this approach has not yet been experimentally validated. Recent studies have indicated that retrons can indeed be leveraged to express functional ssDNA in vivo. For example, Lopez et al tested modifications to the ncRNA in case of retron Eco1 in order to boost RT-DNA abundance[32]. More recently, Liu et al also used retron Eco1 to express 10-23 DNAzyme in vivo[36]. However, it is poorly understood how the encoding of a functional ssDNA sequence in retrons will affect its activity. Such studies may lead to valuable design principles that would be

especially important in the cellular context, as the RT-DNA is known to interact with not only the RT, but, depending on the retron, also RNaseH and the retron associated effector proteins.[24,25]

In this work, we demonstrate the expression of DNA FLAP Lettuce as a model using the *Escherichia coli* retron Eco2[37]. We selected Eco2 as the expression platform due to its reduced complexity compared to other retrons, which could potentially affect the synthesis and folding of the modified RT-DNA. Notably, reverse transcription in the case of retron Eco2 is independent of RNase H.[24] Additionally, the effector protein in retron Eco2 is fused to the RT gene.[26] Using in vitro prototyping we identified suitable integration sites of the aptamer within the retron *msd*. We observe notable differences in aptamer performance between in vitro and intracellular conditions, indicating better aptamer folding in vivo. This suggests that the retron system could be effectively used for the expression and evolution DNA aptamers in living cells.

Results

To obtain an inducible expression system for the retron Eco2 RT-DNA, we performed expression assays with the low copy plasmid pET28a in *E. coli* BL21AI cells and quantified the expression levels (Figure 1). Upon induction of expression with IPTG and arabinose, we observed an ~8-fold increase in RT-DNA levels using qPCR experiments (Figure 2A). This estimate is similar to that of Lopez et al. for Eco1 expression experiments[32]. The intracellular synthesis of Eco2 RT-DNA was furthermore confirmed by denaturing PAGE of DNA extracts, which revealed expression levels that were approximately three to four times higher than those of genomically encoded Eco1 RT-DNA in BL21AI cells (Figure 2B).

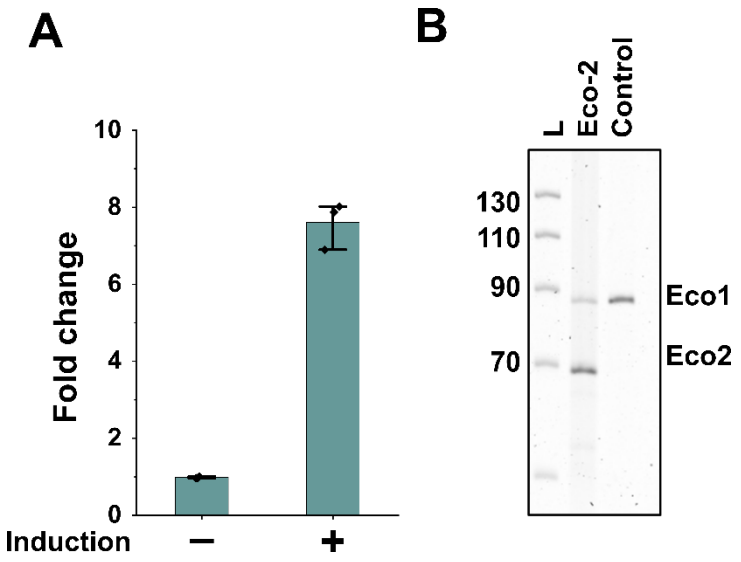

Figure 2. (A) Fold enrichment of the RT-DNA/plasmid template over the plasmid alone upon induction, as measured by qPCR; Unpaired t-test, induced versus uninduced: $p < 0.0001$; n = 3 biological replicates. (B) A TBE-Urea polyacrylamide gel, stained with SYBR Gold showing RT-DNA corresponding to retron Eco1 (90 nt) and retron Eco2 (70 nt).

Having established the inducible expression of plasmid-encoded Eco2 in *E. coli*, we next sought to explore its suitability as a scaffold to host a functional Lettuce aptamer. Expression of ssDNA using retrons is typically achieved by encoding a cargo gene in the *msd* region of the ncRNA. This approach has been successfully demonstrated for recombineering donors[32], protein-binding DNA sequences[38] and DNAzymes[36]. However, it was not clear as to what extent the folding of the cargo aptamer sequence would be affected due to the extensive secondary structure of the Eco2 *msd-msr* RNA-DNA hybrid.

We speculated that the position of the Lettuce aptamer domain in the *msd* region would significantly affect its ability to fold into the functional three-dimensional structure. To test this hypothesis, we used a structure-guided approach to insert a minimized Lettuce variant (4L) into four different positions in the *msd* region of retron Eco2 (Figure 3). 4L has a truncated P1 stem of only 4 bp and is reported to be equally fluorogenic as the full-length Lettuce aptamer[14]. To identify four suitable insertion sites in the *msd*, we used the minimal free energy structure predicted for the Eco2 wild type *msd* by RNAfold[39] with energy parameters for DNA as guide to identify single stranded and / or loop regions where an insertion of the Lettuce domain was expected to not interfere with the native fold of the remaining *msd* sequence. We omitted the *msr*-overlapping region in the input sequences as it is

known to form a duplex with the RT-DNA as well as the *msr* RNA, as to the best of our knowledge, there is no algorithm capable of simulating mixed RNA-DNA sequences that are connected via a 2'-5' bond. The positions v1 and v3 are in two different predicted loop regions. Insertion site v2 is located in a predicted single-stranded region connecting two hairpin loops, while position v4 is just upstream of the predicted base-paired region between the *msd* and *msr* sequences. We designated the constructs corresponding to the 4 distinct positions in the *msd* region as 4LE-v1 to 4LE-v4 (for 4L in Eco2 variant 1-4).

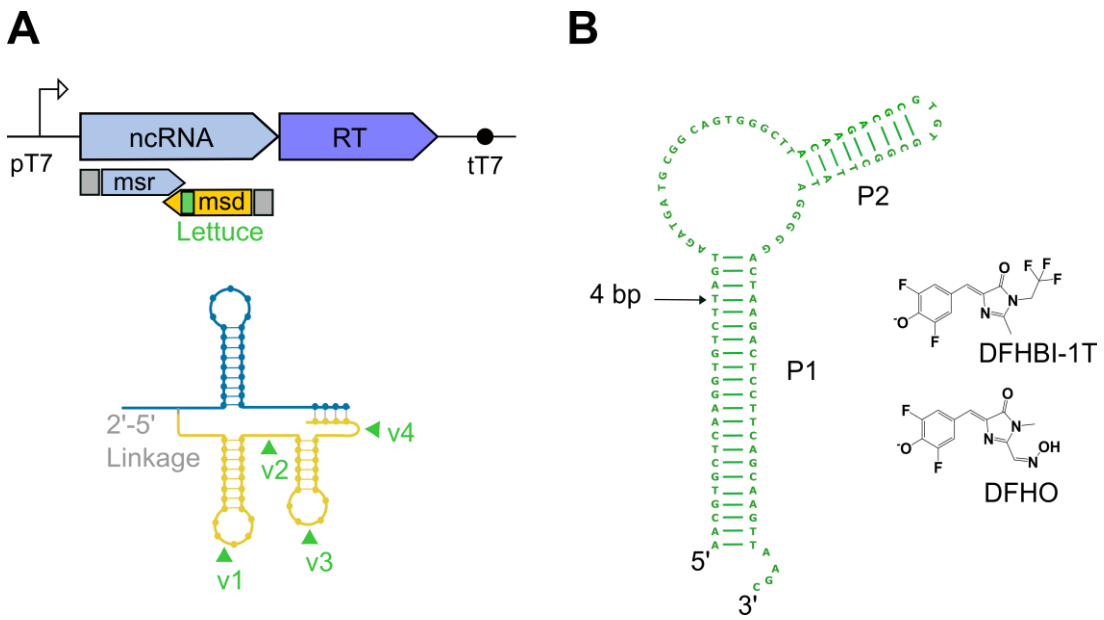

Figure 3. (A) Schematic of insertion of Lettuce aptamer sequence in 4 distinct positions in the *msd* region of retron eco2. (B) Predicted secondary structure of Lettuce aptamer. The arrow indicates the length to which the P1 stem can be shortened without significant loss of FLAP functionality.

To probe if the aptamer domain can still fold after embedding it into the four integration sites of the emulated Eco2 RT-DNA, we determined the dissociation constants between DFHBI-1T and the chemically synthesized 4LE surrogates using the reported Lettuce binding buffer (40 mM HEPES pH 7.5, 100 mM KCl, and 1 mM $MgCl_2$)[14]. When increasing concentrations of the oligonucleotides were incubated in binding buffer containing a constant concentration of DFHBI-1T, we obtained a well-defined fluorescence response for full length Lettuce with the complete P1 stem (Supplementary Figure S1). The data could be well fitted with a quadratic binding equation, resulting in a dissociation constant (K_d) of ~1.5 µM (0.01, 3.89, 95% CI) (Supplementary Figure S1). Binding was weaker for the synthesized ssDNA mimic

4LE-v4 with a K_d of ~20 µM (19, 21.9, 95% CI). The variants 4LEv1, v2 and v3 appeared to be incapable of fluorogenic binding of the DFHBI-1T ligand under the in vitro conditions tested.

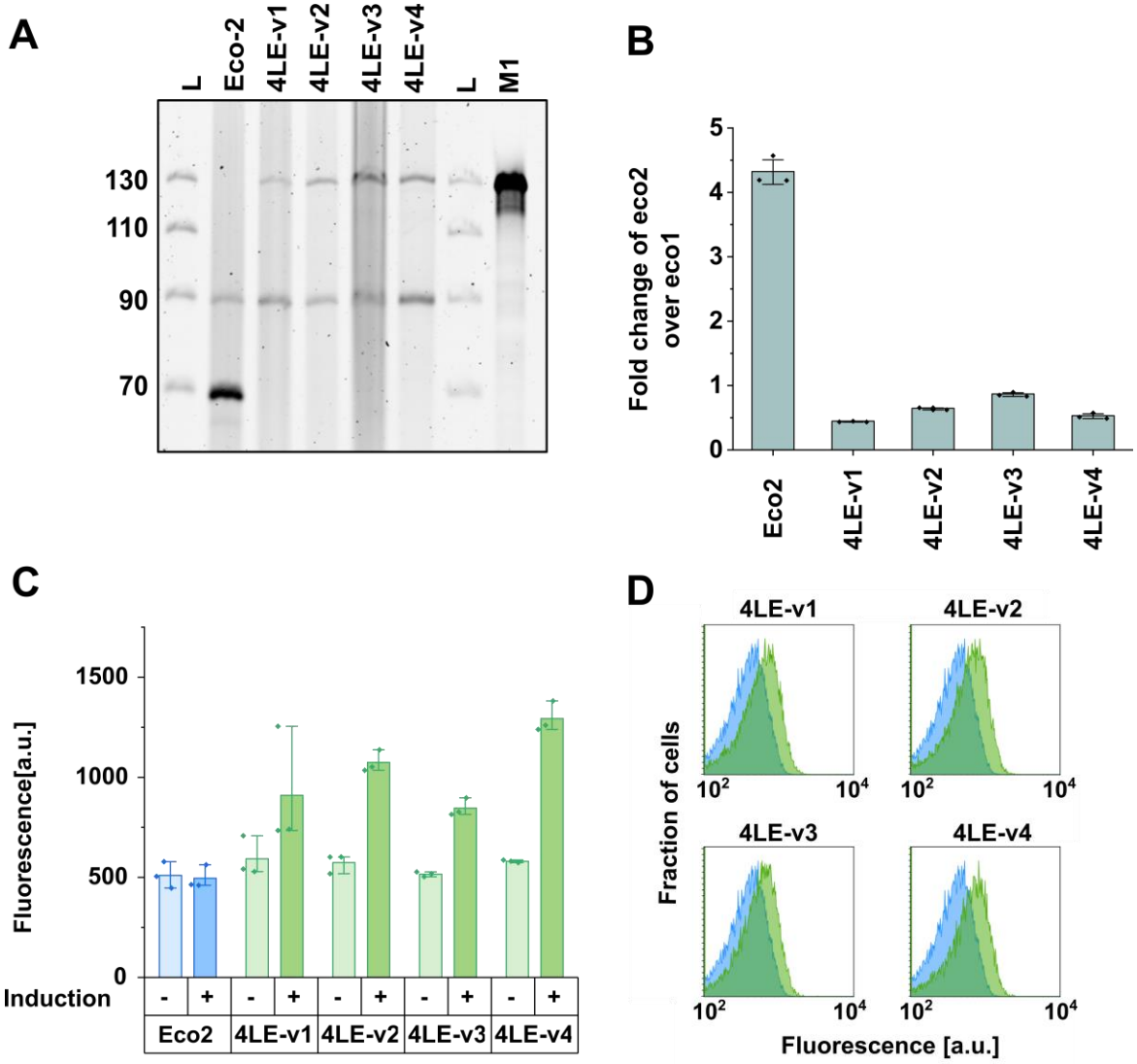

Figure 4. (A) Denaturing PAGE analysis of RT-DNAs extracted from cells expressing either retron Eco2 (67 nt) or 4LE-v1 to v4 (126 nt). Genomically encoded retron Eco1 (90 nt) served as internal control. Marker M1 is a chemically synthesized DNA-version of 4LE-v4. (B) Fold enrichment of RT-DNA corresponding to retron Eco2 (67 nt) and 4LE variants over endogenous Eco1 as determined by length-normalized fluorescence band intensity analysis. Data shown is from n = 3 technical replicates. (C) Bulk in vivo fluorescence measurements with DFHBI-1T. Paired t test, induced versus uninduced: Eco2, p = 0.86; 4LE-v1, p = 0.27; 4LE-v2, p = 0.003; 4LE-v3, p = 0.007; 4LE-v4, p = 0.005; n = 3 biological replicates. (D) Flow cytometry analysis of DFHBI-1T-stained cells expressing 4Lettuce position variants.

Having confirmed that the v4 surrogate construct could induce conditional DFHBI-1T fluorescence, we investigated whether the generated Lettuce variant constructs

could be expressed in *E. coli* after integration into the plasmid-borne *msd* region of retron Eco2 (Figure 4). We were able to verify the full-length synthesis of all four Eco2-4Lettuce variant constructs (126 nt) by PAGE analysis of the isolated RT-DNA (Figure 4A), despite the fact that encoding the 4L aptamer (59 nt) in the *msd* region of retron Eco2 almost doubled the length of the RT-DNA (67 nt). Overall, the insertion of the 4Lettuce aptamer domain into the *msd* region of retron Eco2 resulted in a decrease in RT-DNA level compared to wild-type Eco2: While the wild-type Eco2 *msd* band intensity was 4-fold higher than the endogenous Eco1 band, the four 4LE variant constructs showed 30-70% of the Eco1 expression levels (Figure 4B).

We next investigated the ability of the aptamers to bind DFHBI-1T in cells. To this end, we measured the increase in fluorescence at 520 nm of *E. coli* cells 16 h after induction of the engineered Eco2 operons (Methods, Figure 4C). Using the in vitro binding data as a proxy for DFHBI-1T binding, we hypothesized that 4LE-v4 would show the best binding properties under in vivo conditions, resulting in the highest fluorescence levels, followed by v3. In contrast, we did not expect v1 and v2 to show fluorogenic DFHBI-1T binding in vivo. Indeed, cells expressing the *msd* construct containing 4LE-v4 displayed the most pronounced increase in fluorescence. In case of 4LE-v4, we observed a ~2.6-fold increase compared to background represented by an equivalent number of cells expressing wild type Eco2 and a ~2-fold increase compared to the uninduced sample. Unexpectedly, we also observed 1.7 to 2-fold increases in fluorescence, compared to the negative control (wild type Eco2) in cultures expressing the *msd* constructs 4LE-v1, v2 and v3 (Figure 4C), whose in vitro mimics showed no ligand binding in in vitro measurements.

In experiments using the alternative Lettuce ligand DFHO, we observed a similar trend for 4LE-v4, which showed a 2-fold increase in fluorescence over control cells (Supplementary Figure S2). DFHO is a fluorophore structurally related to DFHBI-1T, with the Lettuce-DFHO complex producing red-shifted fluorescence[14]. We did not observe any increase in fluorescence with DFHO in the case of 4LE-v3. Overall, we found that the relative increase in fluorescence for DFHO was approximately 20% lower than for DFHBI-1T in all expressed variants except 4LE-v3, which showed no increase in fluorescence. This observed difference in fluorescence levels between DFHO and DFHBI-1T is similar to that observed by Passalacqua et al. in in vitro studies.[15] We further confirmed that the increase in fluorescence was a result of

intracellular production of functional Eco2-Lettuce fusion constructs in additional flow cytometry experiments (Figure 4D). Again, a clear increase in green fluorescence was observed in bacteria expressing one of the four 4Lettuce variants compared to cells expressing wild type Eco2.

Discussion

Bacterial retrons such as Eco2 provide a versatile platform for intracellular reverse transcription-based synthesis of single-stranded DNA without causing adverse effects such as triggering the SOS response or viral defense mechanisms. To our knowledge, our present study is the first to show that functional DNA aptamers recognizing small molecule ligands can also be expressed via retrons. Expanding the repertoire of retrons for the expression of DNA aptamers promises to significantly expand the repertoire of functional non-coding DNAs and enable the creation of new sensors and regulators with a wide range of intracellular applications. At the same time, retron platforms provide a direct way to tailor DNA aptamers specifically to intracellular conditions. This is particularly important as our data show that the in vitro properties of DNA aptamer constructs may be a poor predictor of their in vivo performance.

We observed a significant decrease in Eco2 expression levels after integration of the Lettuce domain, suggesting that reverse transcription is hindered by the changes in the *msd* sequence.[32] However, it is noteworthy that although encoding the Lettuce aptamer in retron Eco2 resulted in an ~80% reduction in RT-DNA abundance, this was still sufficient to observe significant fluorescence output. A major advantage of retron-based intracellular synthesis of ssDNA in vivo is its simplicity. The desired sequence can be cloned into the *msd* region of plasmid or genomically encoded retron Eco2. As such, the copy number of the aptamer can readily be tuned by inducer concentration, promoter strength and plasmid copy number.

An ever-increasing number of DNA aptamers have been generated against a wide range of targets, from small molecules to macromolecules to whole cells.[3,40] The retron system used in this work could enable the exploration of cellular applications for this large variety of DNA aptamers. Future research aimed at optimizing intracellular synthesis may also elucidate the conditions under which larger single-

stranded DNAs can be synthesized without compromising reverse transcription and may identify the key factors that influence optimal in vivo folding of cargo sequences.

Methods

Constructs and strains

The retron Eco2 sequence (*msd-msr* and RT) was synthesized by IDT as gblock and cloned into pET28a under control of T7 promoter and *lac* operator. Plasmid assembly was performed using the HiFi DNA Assembly (New England Biolabs) according to the supplier's instructions. The resulting plasmids were transformed into chemically competent *E. coli* Top 10 cells. Plasmid sequences were verified by colony PCR and Sanger sequencing (Microsynth AG). Verified plasmids were then transformed into chemically competent *E. coli* BL21AI cells for further experiments. These cells harbor the genomically encoded retron Eco1 which serves as an internal control and a cassette encoding T7 polymerase driven by arabinose-inducible araBAD promoter. Lettuce variant sequences were cloned into retron Eco2 plasmid using Q5® Site-Directed Mutagenesis Kit (New England Biolabs). Primer sequences and annealing temperatures were generated using the NEBaseChanger™ tool.

RT-DNA extraction and gel electrophoresis

5 ml cultures of BL21AI cells with corresponding Lettuce constructs (LB with selection antibiotic) were inoculated with cells from a single colony and grown at 37°C, 220 rpm for 90 min. They were then induced with 1 mM IPTG and 0.2% arabinose, followed by overnight expression. OD_{600} of the overnight culture was measured and cells corresponding to 2 ml of OD_{600} = 1 were used for miniprep. A NEB Monarch® Plasmid Miniprep Kit was used for RT-DNA extraction (New England Biolabs). Following miniprep, cells were eluted in 40 µl milliQ purified water. The miniprep product was then treated with a RNase Cocktail™ Enzyme Mix (Invitrogen) at 37°C for 30 min. The RNase treated samples were then purified using a ssDNA/RNA Clean & Concentrator kit (Zymo).

The purified RT-DNA was analyzed on a 10% TBE-Urea polyacrylamide gel with a 1x TBE running buffer. Gels were stained with SYBR Gold (Invitrogen) and imaged on Sapphire Biomolecular Imager (Azure biosystems). Band intensities were normalized by length of RT-DNA. RT-DNA abundance of Eco2 and Lettuce variants was

quantified by determining fold-change compared to the Eco1 band. Band intensity analysis was performed with ImageJ[41].

qPCR

qPCR experiments were performed using Techne Prime Pro 48 Real-Time qPCR system, according to comparative C_T method,[42,43] as described by Lopez et al.[32] For qPCR analysis, cell cultures grown for ~16h were used. 25 µl of bacterial culture at an OD_{600} = 1 was mixed with 25 µl water and incubated at 95°C, for 5 min to lyse cells. 0.3 µl of this boiled culture was used as templates in 30 µl qPCR reactions using Luna® Universal qPCR Master Mix (New England Biolabs). qPCR quantification of RT-DNA abundance was performed using a set of three primers. Two primers were complementary to the *msd* region of Retron Eco2 and the third was an outnest primer complementary to non-retron elements of the expression plasmid. Two templates were thus amplified: One corresponding to an RT-DNA sequence that could use both the RT-DNA and the plasmid as templates, and a second that could use only the RT-DNA of Eco2 as a template. The difference between cycle threshold (ΔC_T) of the inside (RT-DNA) and outside (plasmid) primer sets was then calculated. This ΔC_T was then subtracted from the ΔC_T of uninduced samples. Fold enrichment of RT-DNA/plasmid over plasmid alone was then calculated as $2^{-\Delta\Delta C_T}$, for each biological replicate. Presence of RT-DNA results in a fold change > 1.

In vivo fluorescence measurements

25 ml cultures (LB with selection antibiotic) were seeded with a colony and grown at 37°C, 220 rpm for 90 min in a 250 ml baffled flask. They were then induced with 1 mM IPTG and 0.2% arabinose, followed by growth for ~16 h. Culture volume corresponding to 4 ml of OD_{600} = 1 culture was pelleted and washed twice with 1 ml 1x PBS. The pellet was then resuspended in 400 µl 1x PBS and 40 µM DFHBI-1T was added to the cell suspension, followed by incubation at room temperature for 20 min. The stained cells were then used for plate reader and flow cytometry measurements. Plate reader measurements were performed with a BMG Labtech Clariostar plus plate reader at excitation and emission wavelengths of 470 nm and 520 nm, respectively.

Flow cytometry measurements of the Lettuce variants was conducted on a SH800S Cell Sorter (Sony Biotechnology) equipped with 488 nm, 405 nm, 638 nm, and 561

nm lasers, alongside a 100 µm microfluidic sorting chip (Sony Biotechnology). The "Optical Filter Pattern 2", whereby only the 488 nm laser was utilized, was suitable for the detection of Lettuce-DFHB1-1T fluorescence in FL2 at 50.7 % PMT. Exclusively regular cells from a control population were analyzed. This selection was based on a forward scatter intensity of 16 a.u. and a PMT setting of 35 % for the backward scatter. Prior to analysis, the samples were pipetted up and down to ensure a homogeneous suspension. Each Lettuce variant was evaluated by 50,000 events.

Competing Interest Statement

The authors declare no competing interest.

Author Contributions

M.V., C.M., D.S., H.M. designed research; M.V., C.M., S.K. performed research; M.V., C.M., K.B., H.M., analyzed data; K.B. contributed new reagents/analytic tools; and M.V. and H.M wrote the paper.

Author ORCIDs

Mahesh A. Vibhute https://orcid.org/0000-0002-5230-5290
Katrin Bigler https://orcid.org/0000-0003-3737-229X
Daniel Summerer https://orcid.org/0000-0002-3019-7241
Hannes Mutschler http://orcid.org/0000-0001-8005-1657

Acknowledgements

The authors would like to thank Indrayani Phadtare and members of Mutschler lab for fruitful discussions. HM acknowledges support by the European Research Council (ERC) under the Horizon 2020 research and innovation program (grant agreement ID: 802000, RiboLife).

References

1. Dunn, M. R., Jimenez, R. M. & Chaput, J. C. Analysis of aptamer discovery and technology. *Nat. Rev. Chem.* **1,** 1–16; 10.1038/s41570-017-0076 (2017).

2. Keefe, A. D., Pai, S. & Ellington, A. Aptamers as therapeutics. *Nat. Rev. Drug. Discov.* **9,** 537–550; 10.1038/nrd3141 (2010).

3. Qian, S., Chang, D., He, S. & Li, Y. Aptamers from random sequence space: Accomplishments, gaps and future considerations. *Anal. Chim. Acta* **1196,** 339511; 10.1016/j.aca.2022.339511 (2022).

4. Neubacher, S. & Hennig, S. RNA Structure and Cellular Applications of Fluorescent Light-Up Aptamers. *Angew. Chem., Int. Ed.* **58,** 1266–1279; 10.1002/anie.201806482 (2019).

5. Zhou, H. & Zhang, S. Recent Development of Fluorescent Light-Up RNA Aptamers. *Crit. Rev. Anal. Chem.* **52,** 1644–1661; 10.1080/10408347.2021.1907735 (2022).

6. Ouellet, J. RNA Fluorescence with Light-Up Aptamers. *Front. Chem.* **4,** 29; 10.3389/fchem.2016.00029 (2016).

7. Chen, X. *et al.* Visualizing RNA dynamics in live cells with bright and stable fluorescent RNAs. *Nat. Biotechnol.* **37,** 1287–1293; 10.1038/s41587-019-0249-1 (2019).

8. Paige, J. S., Wu, K. Y. & Jaffrey, S. R. RNA mimics of green fluorescent protein. *Science* **333,** 642–646; 10.1126/science.1207339 (2011).

9. Filonov, G. S., Moon, J. D., Svensen, N. & Jaffrey, S. R. Broccoli: rapid selection of an RNA mimic of green fluorescent protein by fluorescence-based selection and directed evolution. *J. Am. Chem. Soc.* **136,** 16299–16308; 10.1021/ja508478x (2014).

10. Song, W. *et al.* Imaging RNA polymerase III transcription using a photostable RNA-fluorophore complex. *Nat. Chem. Biol.* **13,** 1187–1194; 10.1038/nchembio.2477 (2017).

11. Dolgosheina, E. V. *et al.* RNA mango aptamer-fluorophore: a bright, high-affinity complex for RNA labeling and tracking. *ACS Chem. Biol.* **9,** 2412–2420; 10.1021/cb500499x (2014).

12. Dey, S. K. *et al.* Repurposing an adenine riboswitch into a fluorogenic imaging and sensing tag. *Nat. Chem. Biol.* **18,** 180–190; 10.1038/s41589-021-00925-0 (2022).

13. Zhu, Q., Liu, G. & Kai, M. DNA Aptamers in the Diagnosis and Treatment of Human Diseases. *Molecules* **20,** 20979–20997; 10.3390/molecules201219739 (2015).

14. VarnBuhler, B. S., Moon, J., Dey, S. K., Wu, J. & Jaffrey, S. R. Detection of SARS-CoV-2 RNA Using a DNA Aptamer Mimic of Green Fluorescent Protein. *ACS Chem. Biol.* **17,** 840–853; 10.1021/acschembio.1c00893 (2022).

15. Passalacqua, L. F. M. *et al.* Intricate 3D architecture of a DNA mimic of GFP. *Nature* **618,** 1078–1084; 10.1038/s41586-023-06229-8 (2023).

16. Mou, Y. *et al.* Engineering of An Aptamer-Functionalized Fluorescent DNA Sensor for Cu(II) Responding in Living Tumor Cells. *Anal. Chem.* **95,** 8348–8356; 10.1021/acs.analchem.3c01008 (2023).

17. Lin, C. *et al.* In vivo cloning of artificial DNA nanostructures. *Proc. Natl. Acad. Sci. U. S. A.* **105,** 17626–17631; 10.1073/pnas.0805416105 (2008).

18. Chen, F. *et al.* A novel replicating circular DNAzyme. *Nucleic Acids Res.* **32,** 2336–2341; 10.1093/nar/gkh547 (2004).

19. Li, J., Wang, N., Luo, Q. & Wan, L. The 10-23 DNA enzyme generated by a novel expression vector mediate inhibition of taco expression in macrophage. *Oligonucleotides* **20,** 61–68; 10.1089/oli.2009.0217 (2010).

20. Chen, Y., Ji, Y.-J. & Conrad, C. Expression of ssDNA in mammalian cells. *BioTechniques* **34,** 167–171; 10.2144/03341dd04 (2003).

21. Chen, Y. A novel single-stranded DNA expression vector. *Expert Opin. Biol. Ther.* **2,** 735–740; 10.1517/14712598.2.7.735 (2002).

22. Elbaz, J., Yin, P. & Voigt, C. A. Genetic encoding of DNA nanostructures and their self-assembly in living bacteria. *Nat. Commun.* **7,** 11179; 10.1038/ncomms11179 (2016).

23. Alon, D. M., Voigt, C. A. & Elbaz, J. Engineering a DNAzyme-Based Operon System for the Production of DNA Nanoscaffolds in Living Bacteria. *ACS Synth. Biol.* **9,** 236–240; 10.1021/acssynbio.9b00415 (2020).

24. Palka, C., Fishman, C. B., Bhattarai-Kline, S., Myers, S. A. & Shipman, S. L. Retron reverse transcriptase termination and phage defense are dependent on host RNase H1. *Nucleic Acids Res.* **50,** 3490–3504; 10.1093/nar/gkac177 (2022).

25. Wang, Y. *et al.* Cryo-EM structures of Escherichia coli Ec86 retron complexes reveal architecture and defence mechanism. *Nat. Microbiol.* **7,** 1480–1489; 10.1038/s41564-022-01197-7 (2022).

26. Millman, A. *et al.* Bacterial Retrons Function In Anti-Phage Defense. *Cell* **183,** 1551-1561.e12; 10.1016/j.cell.2020.09.065 (2020).

27. Bobonis, J. *et al. Bacterial retrons encode tripartite toxin/antitoxin systems* (Cold Spring Harbor Laboratory, 2020).

28. Simon, A. J., Ellington, A. D. & Finkelstein, I. J. Retrons and their applications in genome engineering. *Nucleic Acids Res.* **47,** 11007–11019; 10.1093/nar/gkz865 (2019).

29. Simon, A. J., Morrow, B. R. & Ellington, A. D. Retroelement-Based Genome Editing and Evolution. *ACS Synth. Biol.* **7,** 2600–2611; 10.1021/acssynbio.8b00273 (2018).

30. Ellington, A. J. & Reisch, C. R. Efficient and iterative retron-mediated in vivo recombineering in Escherichiacoli. *Synth. Biol.* **7,** ysac007; 10.1093/synbio/ysac007 (2022).

31. Schubert, M. G. *et al.* High-throughput functional variant screens via in vivo production of single-stranded DNA. *Proc. Natl. Acad. Sci. U. S. A.* **118**; 10.1073/pnas.2018181118 (2021).

32. Lopez, S. C., Crawford, K. D., Lear, S. K., Bhattarai-Kline, S. & Shipman, S. L. Precise genome editing across kingdoms of life using retron-derived DNA. *Nat. Chem. Biol.* **18,** 199–206; 10.1038/s41589-021-00927-y (2022).

33. Lim, H. *et al.* Multiplex Generation, Tracking, and Functional Screening of Substitution Mutants Using a CRISPR/Retron System. *ACS Synth. Biol.* **9,** 1003–1009; 10.1021/acssynbio.0c00002 (2020).

34. Sharon, E. *et al.* Functional Genetic Variants Revealed by Massively Parallel Precise Genome Editing. *Cell* **175,** 544-557.e16; 10.1016/j.cell.2018.08.057 (2018).

35. Liu, W. *et al.* Retron-mediated multiplex genome editing and continuous evolution in Escherichia coli. *Nucleic Acids Res.* **51,** 8293–8307; 10.1093/nar/gkad607 (2023).

36. Liu, J. *et al.* Generation of DNAzyme in Bacterial Cells by a Bacterial Retron System. *ACS Synth. Biol.* **13,** 300–309; 10.1021/acssynbio.3c00509 (2024).

37. Lampson, B. C. *et al.* Reverse transcriptase in a clinical strain of Escherichia coli: production of branched RNA-linked msDNA. *Science* **243,** 1033–1038; 10.1126/science.2466332 (1989).

38. Lee, G. & Kim, J. Engineered retrons generate genome-independent protein-binding DNA for cellular control. *bioRxiv,* 2023.09.27.556556; 10.1101/2023.09.27.556556 (2023).

39. Lorenz, R. *et al.* ViennaRNA Package 2.0. *Algorithms Mol. Biol.* **6,** 26; 10.1186/1748-7188-6-26 (2011).

40. Sharma, T. K., Bruno, J. G. & Dhiman, A. ABCs of DNA aptamer and related assay development. *Biotechnol. Adv.* **35,** 275–301; 10.1016/j.biotechadv.2017.01.003 (2017).

41. Schindelin, J. *et al.* Fiji: an open-source platform for biological-image analysis. *Nat. Methods.* **9,** 676–682; 10.1038/nmeth.2019 (2012).

42. Livak, K. J. & Schmittgen, T. D. Analysis of relative gene expression data using real-time quantitative PCR and the 2(-Delta Delta C(T)) Method. *Methods* **25,** 402–408; 10.1006/meth.2001.1262 (2001).

43. Schmittgen, T. D. & Livak, K. J. Analyzing real-time PCR data by the comparative C(T) method. *Nat. Protoc.* **3,** 1101–1108; 10.1038/nprot.2008.73 (2008).